Cortical myelin profile variations in healthy aging brain: A T1w/T2w ratio study

Yu Veronica Sui[a,*], **Arjun V. Masurkar**[b,c,d], **Henry Rusinek**[a,e], **Barry Reisberg**[e], **Mariana Lazar**[a]

[a]Department of Radiology, NYU Grossman School of Medicine, 660 1st Ave, rm440, New York, NY 10016, USA

[b]Department of Neurology, Center for Cognitive Neurology, NYU Grossman School of Medicine, New York, NY, USA

[c]Department of Neuroscience and Physiology, NYU Grossman School of Medicine, New York, NY, USA

[d]Neuroscience Institute, NYU Grossman School of Medicine, New York, NY, USA

[e]Department of Psychiatry, NYU Grossman School of Medicine, New York, NY, USA

Abstract

Demyelination is observed in both healthy aging and age-related neurodegenerative disorders. While the significance of myelin within the cortex is well acknowledged, studies focused on intracortical demyelination and depth-specific structural alterations in normal aging are lacking. Using the recently available Human Connectome Project Aging dataset, we investigated intracortical myelin in a normal aging population using the T1w/T2w ratio. To capture the fine changes across cortical depths, we employed a surface-based approach by constructing cortical profiles traveling perpendicularly through the cortical ribbon and sampling T1w/T2w values. The curvatures of T1w/T2w cortical profiles may be influenced by differences in local myeloarchitecture and other tissue properties, which are known to vary across cortical regions. To quantify the shape of these profiles, we parametrized the level of curvature using a nonlinearity index (NLI) that measures the deviation of the profile from a straight line. We showed that NLI exhibited a steep decline in aging that was independent of local cortical thinning. Further examination of the profiles revealed that lower T1w/T2w near the gray-white matter boundary and superficial cortical depths were major contributors to the apparent NLI variations with age. These findings suggest that de-myelination and changes in other T1w/T2w related tissue properties in normal aging may be depth-specific and highlight the potential of NLI as a unique marker of microstructural alterations within the cerebral cortex.

*Corresponding author. veronica.suiyu@nyu.edu (Y.V. Sui).

Keywords

Aging; Myelin sheath; Cerebral cortex; Magnetic resonance imaging

1. Introduction

Myelin is the lipid-rich tissue that ensheaths neuronal axons. It is a crucial component of the human brain due to its role in accelerating neural signaling and promoting synchronization. The thickness of myelin sheath is proportional to axonal diameter, which varies during development and aging (Bouhrara et al., 2021; Michailov et al., 2004). Myelination is thus dynamic across the human lifespan and contributes to activity-dependent neural plasticity (Zatorre et al., 2012). It has been observed that the developmental time course of cerebral myelination follows an inverted U-shape, with the highest myelin content occurring between ages 30 and 60 for different brain regions (Benes et al., 1994; Bouhrara et al., 2020; Grydeland et al., 2013; Yeatman et al., 2014). Myelin abnormalities are at the core of multiple developmental and neurodegenerative disorders (Bartzokis, 2004, 2005; Berry et al., 2020; Papuc and Rejdak, 2020). In normal aging, demyelination is also considered to underlie cognitive decline by disturbing the synchrony of neuronal circuits and slowing down processing speed (Bartzokis, 2004; Papuc and Rejdak, 2020). Degenerated myelin sheaths, both independent of and accompanied by axonal loss, have been reported across gray and white matter regions in non-human primate models of normal aging and were suggested to affect various aspects of brain function (Peters, 2002, 2009).

Approximately 50% of the dry weight of white matter in the mature human brain is myelin (O'Brien and Sampson, 1965). In the cerebral cortex, which contains mostly cell bodies and dendritic spines, myelin is less abundant. However, recent studies have shown that intracortical myelin is strongly associated with brain connectivity (Wei et al., 2018) and is particularly important for the modulation of neural plasticity through its participation in cortical inhibitory neuronal activities (Bartzokis, 2012; Glasser et al., 2014; Micheva et al., 2016). While the majority of *in vivo* myelin studies focus on white matter, the significance of intracortical myelin throughout development and aging is increasingly recognized.

Myelin mapping studies in the neocortex of primates (Bock et al., 2009) have shown a strong correlation between cortical myelin content assessed by histology and T1 and T1-weighted (T1w) images. This is primarily due to the strong effect that tissue macromolecules, which are heavily present in myelin sheath, have on MR signal relaxation described by longitudinal relaxation time (Heath et al., 2018). T2-weighted (T2w) images have also been shown to be inversely correlated to cortical myelin content (Yoshiura et al., 2000), as T2 relaxation rate is affected by tissue iron, which in the cortex is co-localized with myelin content (Fukunaga et al., 2010). Based on these observations, Glasser and van Essen (2011) proposed to use the T1w/T2w ratio for cortical myelin mapping as it both enhances myelin contrast and cancels receive bias field contributions. T1w/T2w ratio in the cerebral cortex has shown good correspondence with known myeloarchitecture and the ability to differentiate cortical areas with distinct myeloarchitectural properties (Glasser et al., 2016; Glasser and Van Essen, 2011; Nieuwenhuys, 2013). It is important to note,

however, that T1w/T2w ratio can be affected by other tissue characteristics that affect T1 and T2 relaxation times, such as the presence of brain iron, edema, and inflammation (Ganzetti et al., 2014; Harkins et al., 2016). It may also be associated with dendrite density in cortical gray matter, which is not necessarily correlated with myelin content (Righart et al., 2017).

As T1w and T2w images are typically part of routine brain MRI exams and can be obtained with high resolution (1mm or less) in relatively short time periods, *in vivo* mapping of intracortical myelin using T1w/T2w ratio has been applied recently to a wide variety of clinical research. However, MRI examinations of cortical myelin in normal aging and neurodegenerative disorders remain limited. Grydeland and colleagues identified an inverted U-shaped path for cortical myelin across lifespan using T1w/T2w ratio and observed negative correlations between myelin and cognitive performance stability in aging (Grydeland et al., 2019, 2013). Using quantitative metrics based on the magnetization transfer effect, Callaghan et al. (2014) reported decreased myelin content in white matter and cerebral cortex with age in healthy participants older than 60. Reduced gray matter/ white matter (GM/WM) contrast was also observed in T1w and T1w/T2w ratio images in Alzheimer's disease (AD) and normal aging (Vidal-Pineiro et al., 2016; Westlye et al., 2009). These findings further implicated the involvement of intracortical myelin changes in aging and pathological neurodegeneration.

A major challenge for intracortical myelin mapping is the laminar organization within the cerebral cortex. Variations in tissue composition across cortical layers and the presence of distinct myelinated fiber bands suggest the need for considering depth-dependent characterizations of intracortical myelin content. To this end, several recent studies have explored sampling cortical profiles perpendicularly through cortical layers (Dinse et al., 2015; Paquola et al., 2019; Sprooten et al., 2019; Sui et al., 2021). Findings from these studies were in line with previous histological reports showing variations in cortical myelin profiles across cortices. More specifically, these studies have suggested that the shape of myelin profiles vary across regions with differences in myelin content (i.e., high versus low myelin), and these variations are associated with local cortical function (Nieuwenhuys, 2013). Studies by our group and others in adolescents and clinical populations further show that the characteristics of cortical myelin profile, such as nonlinearity and skewness, capture subtle layer-specific changes related to development and pathology. These findings highlight the added value of using cortical profiles over the traditional volumetric myelin measures (Paquola et al., 2019; Sprooten et al., 2019; Sui et al., 2021).

In the current study, we employed the recently available Human Connectome Project in Aging (HCP-A) dataset (Bookheimer et al., 2019) with the aim of investigating intracortical myelin alterations in normal aging using a surface-based cortical profile reconstruction approach. We resampled T1w/T2w values along and across surfaces through the entire depth of cerebral cortex based on a percentage-wise method and quantified the shape of these myelin profiles using a single but robust index describing its nonlinearity (the nonlinearity index, NLI). While the current image resolution and artificial surface expansion method do not allow distinction of anatomically meaningful cortical laminae, the T1w/T2w cortical profile approximates the depth-dependent variations in myelin content and related tissue

properties. Our interpretation of results in the following sections will be based on the assumption that cortical T1w/T2w ratio is largely influenced by myelin density. Cortical thickness will be compared and accounted for in the analysis of age-related NLI differences to address potential partial volume effects, as cortical thinning has been robustly observed in aging populations (Shaw et al., 2016). We hypothesize that regional NLI captures variations in the cortical profiles that are distinct from aging related differences in cortical thickness and single-depth T1w/T2w ratio values.

2. Methods

2.1. Imaging data

Datasets from a total of 740 HCP-A participants, including demographic, cognitive, and imaging data, were downloaded from the National Institute of Mental Health Data Archive (NDA) using the provided download manager. Fifteen datasets with missing demographic information (e.g., age and sex) were excluded, leaving 725 datasets for further analysis. HCP-A participants ranged in age from 36 to 100 years, which encompasses mature, aging, and old life stages as categorized by the HCP-A project. In the present study, we defined ages 36-55 as mature, 55-85 as aging, and above 85 as old age groups (Fig. 1a), and we mainly focused on the aging group for the current study. The rationale behind this age segmentation is based on previously reported human brain myelination trajectory which shows an inverted-U shape that peaks approximately within the 30 to 60 years age interval (Benes et al., 1994; Grydeland et al., 2013; Yeatman et al., 2014). Separating ages between 55 and 85 as an aging group therefore enabled us to zoom in on the period of degeneration and describe variations in MRI metrics with age using a linear relationship.

The imaging and behavioral data acquisition procedures of the HCP-A and the structural preprocessing pipelines have been thoroughly described in previous HCP publications (Bookheimer et al., 2019; Glasser et al., 2013; Harms et al., 2018). Briefly, T1w and T2w structural images were acquired on Siemens 3T Prisma scanners using the multi-echo magnetization-prepared rapid gradient echo (MPRAGE; TE = 1.8/3.6/5.4/7.2 ms, TR/TI = 2500/1000 ms, flip angle = 8°, 0.8 mm isotropic voxel size) and the variable flip angle turbo spin-echo (T2w SPACE; TR/TE = 3200/564 ms, 0.8 mm isotropic voxel size) sequences (for the entire imaging protocol, see https://www.humanconnectome.org/study/hcp-lifespan-aging/project-protocol/imaging-protocols-hcp-aging). Our data download employed a limited package (Supplementary Materials Table S1) that contained results of the HCP PreFreeSurfer structural pipeline, which carries out distortion correction, spatial normalization, and bias field correction (Glasser et al., 2013). We then performed surface reconstruction using the HCP *FreeSurferPipeline* on one of our institution's high performance computing platforms with the HCP-recommended FreeSurfer 6.0.0 (Fischl, 2012) and FSL 6.0.4 (Jenkinson et al., 2012).

High resolution T1w/T2w ratio images were generated and used as cortical myelin estimates in the current study. While taking the ratio of T1w and T2w images effectively cancels out the receive field effects, non-negligible transmit bias field effects may remain as they are distinct to each image. Here, we did not use any additional bias field correction as current analysis focuses on the relative shape of cortical profiles within the cortical ribbon, which

due to their localized nature should not be greatly influenced by bias field effects. The bias correction provided in the HCP pipelines that regularizes transmit field bias using smoothed group average T1w/T2w myelin maps was also omitted. Although this correction step was shown to provide more reliable cortical segmentations (Glasser et al., 2016, 2013), it can remove natural variations in T1w/T2w values across participants and thus is not suitable for cross-participants statistical analysis (Glasser et al., 2022;Shams et al., 2019). Since the residual bias field is shown to be correlated to body mass index (BMI) (Glasser et al., 2022), we included the participants' BMI as a covariate in all correlational analyses. Some (Cooper et al., 2019; Ganzetti et al., 2014), but not all (Grydeland et al., 2019; Grydeland et al., 2013; Nakamura et al., 2017) of previous research has also employed additional steps to normalize T1w and T2w images. Here we chose not to perform any additional intensity normalization on the final T1w/T2w myelin maps, since previously proposed methods (Ganzetti et al., 2014; Misaki et al., 2015) utilized intensity values of specific ROIs that may introduce confounding age effects. For instance, the T1w MPRAGE signal intensity of the eyeball (vitreous body), which is one of the reference regions used in Ganzetti et al. (2014), has been shown to significantly increase with age (Streckenbach et al., 2020).

2.2. Depth-specific T1w/T2w and cortical, profile nonlinearity index

The Desikan-Killiany atlas (Desikan et al., 2006) was used for cortical parcellation. Mean cortical thickness (CT) and T1w/T2w ratio for each cortical region of interest (ROI) were extracted using FreeSurfer. Regional T1w/T2w and CT values out of two interquartile ranges below the first or above the third quartile, representing 2.9% of T1w/T2w values and 0.7% of CT values across datasets, were deemed outliers and not used in the analyses. Analyses and results based on a more granular atlas (Glasser et al., 2016) were included in the Supplementary section 3.3 for comparison purpose.

To characterize intracortical T1w/T2w profiles across cortical depths, we sampled T1w/T2w values from 11 surfaces which segmented the cortical ribbon into 10 sections (Fig. 1b). Using FreeSurfer mri_vol2surf, two surfaces near the FreeSurfer defined pial (1% CT deep) and the white matter surface (99% CT deep) along with nine uniformly spaced surfaces (between 10% and 90% CT depths spaced 10% CT apart) were expanded for each subject. The 1% and 99% cortical depths were chosen to mitigate contamination from cerebrospinal fluid or white matter at the cortical ribbon boundaries. T1w/T2w volume resampling was implemented along with surface expansion in the mri_vol2surf command. For each projection fraction, the new surface was expanded and placed by projecting outwards from the white matter surface along the surface normal to the pial surface using the corresponding projection fraction, after which T1w/T2w values were resampled at the expanded surface position using trilinear interpolation. Mean T1w/T2w values were extracted from the expanded 11 surfaces for each cortical ROI using FreeSurfer mri_segstats. This sampling density was chosen to obtain a smooth approximation of the curved profile while avoiding oversampling (see Supplementary Fig. S1). These single-depth values were then used to construct a cortical myelin profile for each region (Fig. 1c).

To quantify the T1w/T2w cortical profile shape of each region, an NLI was calculated as the root-mean-square deviation of the T1w/T2w profile curve from a linear regression line, $\hat{y}(x) = a + bx$ (Fig. 1c):

$$NLI = \sqrt{\frac{\sum_{i=1}^{11} (y_i - \hat{y}_i)^2}{11}} \qquad (1)$$

where i indexes the cortical depths, y_i are the sampled T1w/T2w ratio values across the cortical profile, and $\hat{y}_i$ are the corresponding linearly fitted values.

For standardization, NLI values were subsequently scaled across all datasets and all regions to a mean of 2 and a standard deviation of 1 (Sui et al. 2021). All results below list scaled NLI values. T1w/T2w profiles of all study regions and average NLI across age groups are included in the Supplementary Material (Figs. S2, S3). Since the NLI was calculated from the cortical T1w/T2w values, it had the same 2.9% missing values across all datasets. Data manipulation including outlier removal and NLI calculation were performed in MATLAB (The MathWorks Inc, Natick, MA, USA).

2.3.   Replication study

To understand the generalizability of the HCP-A results, we applied the same structural processing and NLI calculating pipeline to the healthy aging sample from the Cambridge Centre for Ageing and Neuroscience (Cam-CAN; Shafto et al., 2014; Taylor et al., 2017). The partial correlation with age and NLI described in 2.4 were conducted on the Cam-CAN datasets. These results are presented in the Supplementary Materials section 4.

2.4.   Statistical analysis

Statistical analyses and data visualization were performed in MAT-LAB and FreeSurfer. Descriptive statistics of participants' age, sex, and BMI were calculated by age groups (Table 1). While the focus of the study is the aging group, for the purpose of confirming the inverted-U shape trajectories observed in previous studies using T1w/T2w at 70% cortical depth (Grydeland et al., 2019) in the HCP-A dataset, we tested the quadratic age effect in T1w/T2w at the same depth across participants of all ages. Participants' age, sex, BMI, and local cortical thickness were included as covariates in the quadratic age effect regression analysis.

In the aging group, Pearson's correlation and linear regression were used to test age-related variations in regional NLI and CT, and T1w/T2w values at specific depth. To test if the NLI captures age-related variations that are independent of CT differences, partial correlations were used to account for regional CT. Finally, mediation analyses (Baron and Kenny, 1986) were conducted to assess the mediation effect of T1w/T2w values at specific depth on NLI variations in aging, controlling for the variations in CT. Subjects' age and NLI were treated as predictor and outcome variables respectively, and T1w/T2w values at superficial (average T1w/T2w from outmost 20% cortical sections), middle (T1w/T2w at 50% cortical depth), and inner sections (average T1w/T2w from deep 20% cortical sections near white matter) were tested as the mediator. The mediation analysis was performed in each region

separately with the mediation effect quantified by the percentage mediated, calculated as the ratio of the effect accounted for by the pathway through the mediator to the total effect of the predictor (Supplementary 3.2; Fig. S6). Participants' sex and BMI were included as covariates in all correlation and mediation analyses described above. Bonferroni correction was used when applicable to correct for multiple comparisons across the 68 cortical ROIs. Results were considered significant at a corrected p (p^*) smaller than 0.05 (equivalent to an uncorrected p of 0.00074).

3. Results

Across all age groups, T1w/T2w at 70% cortical depth showed significant quadratic age effects in ROIs across the prefrontal, temporal, and parietal area (Figs. 2a, S4; Table S2). No significant age and sex interaction was noted in the regression analysis. Pearson's correlation across bilateral cortical ROIs revealed a significant inverse relationship between the NLI and T1w/T2w ratio at 70% depth (Fig. 2b). In the aging group specifically (Fig. 3), higher average T1w/T2w at 70% depth were observed in primary cortices including the occipital lobe and parietal lobe, particularly sensorimotor area along the central sulcus. Association areas such as the prefrontal, cingulate, and most of the temporal regions showed relatively lower T1w/T2w (Fig. 3a). In contrast, NLI magnitude across the cortical surface exhibited the opposite pattern, with lower NLI found in most of the primary cortices and higher NLI found in the prefrontal, cingulate and inferior temporal regions (Fig. 3b).

In the aging group, both CT and the NLI showed significant negative associations with age in majority of cortical regions (Fig. 4; Table S3). In limited ROIs along the central sulcus, significant positive correlations with age were also noted for NLI. Results from partial correlations between NLI and age adjusting for CT variations indicated that NLI variations in the aging group were robust and independent of local CT reductions (Fig. 5; Table S3). Bilateral prefrontal, cingulate, and lower temporal regions were among the ones that showed the steepest NLI decreases with age controlling for regional CT and the covariates (Fig. 5b).

To further understand the mechanism behind the observed NLI variations in aging, we inspected regional T1w/T2w profiles of participants on the younger (ages 55-60) against the older (ages 80-85) side of the aging group (Fig. 6a). Profile differences appear to concentrate near the pial and white matter surfaces, which leads to lower NLI values in regions with relatively nonlinear profiles in the mature group and slightly higher NLI in linear regions such as the precentral region. To visualize age-related changes in cortical profiles, we displayed individual T1w/T2w profiles colored according to participants' age and centered the profiles at T1w/T2w values at 50% depth (Fig. 6b), given that no T1w/T2w variations with age at this depth exceeded statistical significance after multiple comparison correction in most brain regions (Table S4). Following mediation analyses confirmed that lower T1w/T2w at the deepest 20% section within the cortical ribbon (described by averaging T1w/T2w values at 80%, 90%, and 99% cortical thickness depths, near the white surface) and the most superficial 20% (near the pial surface) were the main contributors to age-related NLI variations (Fig. 6c). The average T1w/T2w at the deep cortical depth mediated NLI variations in 52 bilateral ROIs, and this mediation pathway explained up to 45% of age-related variance in regional NLI after controlling for participants' sex, BMI,

and regional CT. The mediation effect of T1w/T2w at the superficial cortical depth was relatively moderate and explained up to 16% of NLI age effects in 7 ROIs after controlling for the covariates. Finally, mid-thickness T1w/T2w (at 50% depth) in the left transverse temporal region was significantly higher with older age, which explained 16% of regional NLI variations (Fig. 6c; Table S4). This finding at 50% depth was not statistically significant in any other cortical ROIs in the aging group.

4. Discussion

The current study revealed distinct intracortical T1w/T2w profile alterations in normal aging, which may reflect myeloarchitectural and depth-specific cortical changes in older age. To describe the laminar organization of the cerebral cortex, we generated T1w/T2w profiles and characterized myeloarchitectural variation patterns of each region using NLI. We found that age-related NLI variations in the cortical myelin profile were more extensive throughout the cerebral cortex than CT differences. More importantly, these variations in profile shape remained significant when regional CT was adjusted for, highlighting the added value of characterizing cortical myelin profile NLI in studying lifespan changes as well as this metric's independence of atrophy. These findings were shown to be reproducible in the Cam-CAN dataset, which had a similar healthy aging sample and a slightly different imaging protocol (see Supplementary materials section 4). Further examinations of the profiles revealed marked T1w/T2w reductions near the GM/WM boundary and pial surface, particularly the former. This observation was corroborated by mediation analyses, which showed that a significant portion of NLI variation with age was explained by lower T1w/T2w at specific cortical depths. Overall, these results suggest that myelin and T1w/T2w related tissue properties at different cortical depth may be affected non-uniformly in normal aging.

Consistent with previous histological and MRI findings on intracortical myelin distribution (Glasser et al., 2014; Nieuwenhuys, 2013; Stuber et al., 2014), in heavily myelinated primary cortices such as the sensorimotor and primary visual areas, we observed higher and relatively linearly increasing T1w/T2w within the cortical ribbon, and therefore low NLI. In comparison, association cortices including the prefrontal and cingulate regions showed lower T1w/T2w values and more nonlinear profiles (Figs. 2b, 3). Across all age groups, we also replicated the quadratic age effect in T1w/T2w, primarily in the cingulate, temporal, and prefrontal regions (Fig. 2a, S4; Table S2). The trajectories of myelination (either inverted U-shaped or linear-shaped) in multiple ROIs are comparable to previously reported findings of cortical myeli-nation across lifespan (Benes et al., 1994; Grydeland et al., 2013), in terms of both trajectory curvature and peak location.

Myelin degeneration has been found in the aging brain through histological studies in the form of ultrastructural abnormalities in myelin sheath and myelin breakdown (Peters, 2009). Lintl and Braak (1983) reported marked myelin loss in the visual cortex starting as early as the third decade of life. In the current study, we found that for participants aged between 55 and 85, regions across prefrontal, temporal, and cingulate cortices showed the steepest NLI decreases (Fig. 5b) and more prominent T1w/T2w decreases, particularly in deep cortical sections, adjusted for CT variations (Fig. 6). The variations observed in cortical

T1w/T2w profile here indicate that cortical myelin, among other tissue properties, may go through age-related changes that are non-uniform across cortical depths. This interpretation is in line with previous histological findings of cortical myelination in both aging and development. Myelin staining data have suggested various degrees of myelin loss across cortical layers with aging (Kemper, 1994). Non-uniform myelination was also observed during development, with myelin content increases from infancy to adulthood appearing to be more prominent in deep cortical layers than in the superficial ones (Miller et al., 2012). It is nevertheless important to note that neither myelin staining nor T1w/T2w values provides quantitative measurements of cortical myelin. The extensively decreased T1w/T2w values from surfaces near the white matter across extended cortical regions observed here may also reflect both localized myelin degeneration and accumulated loss of myelinated fibers from other layers, given that all efferent and afferent fibers in the cerebral cortex travel through deep cortical layers (Nieuwenhuys, 2013). This finding could further reflect in part changes in the adjacent white matter, as previous studies have shown that GM/WM contrast decreases with aging are likely due to reduced T1w/T2w intensity in white matter regions (Colmenares et al., 2021; Vidal-Pineiro et al., 2016).

Intracortical myelin has been suggested to be particularly important in calibrating the synchrony of neural networks as signals travel through cortical layers that are myelinated to various degrees (Haroutunian et al., 2014). Altered cortical myelin profiles and decreased myelin content in normally highly myelinated deep layers in frontal and temporal areas may thus contribute to the overall cognitive decline seen in aging. Based on previously proposed mechanisms, the reduced myelin content in the deep cortical layers and the decreased CT seen here may arise from damaged or thinned myelin sheaths, decreased numbers of certain types of neurons, varied density and organization of dendritic spines, loss of oligodendrocytes, or a combination these processes (Bartzokis, 2004; Lintl and Braak, 1983; Petracca et al., 2020; Rowley et al., 2015).

The current results also resonate with previous findings in clinical populations. In a recent study characterizing the thickness of highly myelinated deep-cortical layers in psychiatric patients (Rowley et al., 2015), the authors suggest that myelin integrity in deep cortical layers plays a particularly critical role in the integration of cortical and subcortical white matter, which in turn affects cognitive performance. More interestingly, the regions found to show greater NLI changes in the aging group here, including the prefrontal and temporal areas, are also frequently implicated in AD neuropathology. Decreased functional connection between prefrontal cortex and hippocampus-related temporal regions has been reliably observed in AD patients, which is suggested to be partly contributed by myelin breakdown and to underlie impaired memory (Bartzokis, 2004; Grady et al., 2001). Recent studies have also shown more direct association of intracortical myelin integrity with both functional (Huntenburg et al., 2017) and structural connectivity (Wei et al., 2018). Therefore, future studies will need to examine whether changes in intracortical myeloarchitecture observed in current healthy aging sample predispose individuals to further myelin and functional deficits in AD.

Of note, cortical T1w/T2w ratio has been found to correlate with amyloid β deposits in cognitively normal individuals aged between 55 and 85 years (Yasuno et al., 2017). In

another study, higher T1w/T2w values were observed in patients with Alzheimer's disease compared to healthy controls (Pelkmans et al., 2019). Indeed, demyelination (i.e., lower T1w/T2w) and amyloid accumulation (i.e., higher T1w/T2w) are processes commonly observed in both normal aging and age-related neurodegenerative diseases. However, no data to date describe how T1w/T2w ratio is affected by these two competing mechanisms. It would therefore be important for future studies to consider these factors when employing T1w/T2w in aging and neurodegenerative disease research to further investigate and potentially utilize the connections between these mechanisms.

Studying myelination across lifespan using MRI has advantages in data acquisition and research scope compared to histological studies, which may be limited by sample size and biased by variation in brain fixation methods (Peters, 2002; Seifert et al., 2019; Shatil et al., 2018). However, the laminar organization of the cerebral cortex poses a major challenge to cortical myelin mapping using MRI: the relative thickness of each layer varies across cortices and regions such as the sensory motor area can greatly deviate from the standard six-layer architecture (Kiernan and Rajakumar, 2013; Nieuwenhuys, 2013). The current approach, which employs a metric that describes the shape of the cortical profiles, appears to capture fine changes in myeloarchitecture while also minimizing multiple comparison problems at initial stages of the analysis. Previous work from our group using a quantitative magnetization transfer method in young adults with schizophrenia spectrum disorders also observed NLI changes in the cortical myelin profile in patients, which were shown to be primarily determined by increased myelin in midcortical depth (Sui et al., 2021). Overall, findings from the current and previous studies using cortical profiles in detecting intracortical myeloarchitecture changes suggest the value of this approach in complementing traditional volumetric methods.

Several important limitations need to be considered when interpreting our results. First, T1w/T2w ratio is not a quantitative measure and can be affected by acquisition parameters and tissue properties besides myelin as mentioned earlier (Glasser et al., 2014; Righart et al., 2017). Of particular note, while cortical layer-specific variations in iron content was previously found to strongly correlated to myelin stain variations (Fukunaga et al., 2010), iron that is not colocalized with myelin lipids will affect MRI signals in T1w and T2w images (Ogg and Steen, 1998) and confound myelin mapping using T1w/T2w ratio. Moreover, previous studies in white matter found that T1w/T2w shared limited amount of variance with relatively myelin-specific markers such as myelin water fraction and magnetization transfer based metrics (Arshad et al., 2016; Hagiwara et al., 2018; Uddin et al., 2019). Other methodological issues of current application of T1w/T2w include potential biases from residual B1 transmit field and intensity variations across scans (Ganzetti et al., 2014; Glasser et al., 2022). We also chose to not include normalization steps that may indirectly reduce or alter brain aging effects as discussed in Methods 2.1. Therefore, while cortical T1w/T2w was found to present similar developmental trajectory and regional distribution that are in line with previous findings of cortical myelination (Benes et al., 1994; Grydeland et al., 2013), caution should be used when interpreting current results as quantitative changes in myelin content. The cross-sectional design of the HCP dataset also limits the interpretation of aging-related variations reported in the current study, as

the possibility of a cohort effect cannot be ruled out and variation with age may reflect differences in the sample composition rather than a change over time.

Additionally, given the limited voxel resolution relative to cortical thickness, the T1w/T2w values obtained at different cortical depths and employed to derive the NLI were an estimation from interpolated values along the surface normal. Thus, they may not accurately reflect myelin content at the exact cortical layer. The relatively dense sampling used here (i.e., expanding 11 surfaces) was chosen to discretize the cortical profile for NLI calculation. The obtained profile is therefore only a smoothed version of the real profile and is unlikely to capture fine variations in T1w/T2w with cortical depth beyond the prescribed resolution. Nonetheless, this study presents a framework for analyzing depth-related variations in cortical myelin content that can be further refined in the future using higher resolution images and parametric maps obtained using higher field strengths or improved acquisition hardware and software. The precision of surface sampling and the accuracy of tissue gradient characterization may also be improved by employing algorithms that compensate for cortical folding, such as the ones implemented in the Connectome Workbench (https://www.humanconnectome.org/software/workbench-command/-surface-cortex-layer). By controlling for CT in our analyses, we aimed to address and control the effect of partial volume averaging. It is worth noting, however, that apparent CT may be dependent on the GM/WM contrast and myelination near the GM/WM boundary (Natu et al., 2019; Westlye et al., 2009). Therefore, current results of cortical changes reflected by altered NLI and decreased T1w/T2w from surfaces near the white matter could also be affected by potential shifts of the apparent GM/WM boundary.

Lastly, as a future direction, it will be useful to apply this cortical profile approach with atlases that are directly based on cytoarchitecture or functional connectivity (Ding et al., 2016; Schaefer et al., 2018; Yeo et al., 2011) accompanied with higher resolution acquisitions. Adapting this method to quantitative measures of myelin content or other tissue properties (Does, 2018; Mezer et al., 2013; Yarnykh, 2012) will also be important to further understand intracortical myelin and microstructural changes in development and aging.

Supplementary Material

Refer to Web version on PubMed Central for supplementary material.

Acknowledgements

Data availability statement

Data used in the preparation of this manuscript were collected as part of the Human Connectome Project in Aging (U01AG052564 and U01AG052564-S1) and are available on the National Institute of Mental Health (NIMH) Data Archive (NDA) at https://nda.nih.gov.

Data availability

Data will be made available on request.

Abbreviations:

NLI   Nonlinearity index

CT   Cortical thickness

References

Arshad M, Stanley JA, Raz N, 2016. Adult age differences in subcortical myelin content are consistent with protracted myelination and unrelated to diffusion tensor imaging indices. Neuroimage 143, 26–39. doi:10.1016/j.neuroimage.2016.08.047. [PubMed: 27561713]

Baron RM, Kenny DA, 1986. The moderator-mediator variable distinction in social psychological research: conceptual, strategic, and statistical considerations. J. Personal. Soc. Psychol 51 (6), 1173–1182. doi:10.1037//0022-3514.51.6.1173.

Bartzokis G, 2004. Age-related myelin breakdown: a developmental model of cognitive decline and Alzheimer's disease. Neurobiol. Aging 25 (1), 5–18. doi:10.1016/j.neurobiolaging.2003.03.001. [PubMed: 14675724]

Bartzokis G, 2005. Brain myelination in prevalent neuropsychiatric developmental disorders: primary and comorbid addiction. Adolesc. Psychiatry 29, 55–96. Retrieved from https://www.ncbi.nlm.nih.gov/pubmed/18668184 . [PubMed: 18668184]

Bartzokis G, 2012. Neuroglialpharmacology: myelination as a shared mechanism of action of psychotropic treatments. Neuropharmacology 62 (7), 2137–2153. doi:10.1016/j.neuropharm.2012.01.015. [PubMed: 22306524]

Benes FM, Turtle M, Khan Y, Farol P, 1994. Myelination of a key relay zone in the hippocampal formation occurs in the human brain during childhood, adolescence, and adulthood. Arch. Gen. Psychiatry 51 (6), 477–484. doi:10.1001/arch-psyc.1994.03950060041004. [PubMed: 8192550]

Berry K, Wang J, Lu QR, 2020. Epigenetic regulation of oligodendrocyte myelination in developmental disorders and neurodegenerative diseases. F1000Res 9. doi:10.12688/f1000research.20904.1.

Bock NA, Kocharyan A, Liu JV, Silva AC, 2009. Visualizing the entire cortical myelination pattern in marmosets with magnetic resonance imaging. J. Neurosci. Methods 185 (1), 15–22. doi:10.1016/j.jneumeth.2009.08.022. [PubMed: 19737577]

Bookheimer SY, Salat DH, Terpstra M, Ances BM, Barch DM, Buckner RL, … Yacoub E, 2019. The lifespan human connectome project in aging: an overview. Neuroimage 185, 335–348. doi:10.1016/j.neuroimage.2018.10.009. [PubMed: 30332613]

Bouhrara M, Kim RW, Khattar N, Qian W, Bergeron CM, Melvin D, … Spencer RG, 2021. Age-related estimates of aggregate g-ratio of white matter structures assessed using quantitative magnetic resonance neuroimaging. Hum. Brain Mapp 42 (8), 2362–2373. doi:10.1002/hbm.25372. [PubMed: 33595168]

Bouhrara M, Rejimon AC, Cortina LE, Khattar N, Bergeron CM, Ferrucci L, … Spencer RG, 2020. Adult brain aging investigated using BMC-mcDESPOT-based myelin water fraction imaging. Neurobiol. Aging 85, 131–139. doi:10.1016/j.neurobiolaging.2019.10.003. [PubMed: 31735379]

Callaghan MF, Freund P, Draganski B, Anderson E, Cappelletti M, Chowdhury R, … Weiskopf N, 2014. Widespread age-related differences in the human brain microstructure revealed by quantitative magnetic resonance imaging. Neurobiol. Aging 35 (8), 1862–1872. doi:10.1016/j.neurobiolaging.2014.02.008. [PubMed: 24656835]

Colmenares AM, Voss MW, Fanning J, Salerno EA, Gothe NP, Thomas ML, … Burzynska AZ, 2021. White matter plasticity in healthy older adults: the effects of aerobic exercise. Neuroimage 239, 118305. [PubMed: 34174392]

Cooper G, Finke C, Chien C, Brandt AU, Asseyer S, Ruprecht K, … Scheel M, 2019. Standardization of T1w/T2w ratio improves detection of tissue damage in multiple sclerosis. Front. Neurol 10 (334). doi:10.3389/fneur.2019.00334.

Desikan RS, Segonne F, Fischl B, Quinn BT, Dickerson BC, Blacker D, … Killiany RJ, 2006. An automated labeling system for subdividing the human cerebral cortex on MRI scans i nto gyral based regions of i nterest. Neuroimage 31 (3), 968–980. doi:10.1016/j.neuroimage.2006.01.021. [PubMed: 16530430]

Ding SL, Royall JJ, Sunkin SM, Ng L, Facer BAC, Lesnar P, … Lein ES, 2016. Comprehensive cellular-resolution atlas of the adult human brain. J. Comp. Neurol 524 (16), 3127–3481. doi:10.1002/cne.24080. [PubMed: 27418273]

Dinse J, Hartwich N, Waehnert MD, Tardif CL, Schafer A, Geyer S, … Bazin PL, 2015 A cytoarchitecture-driven myelin model reveals area-specific signatures in human primary and secondary areas using ultra-high resolution *in-vivo* brain MRI. Neuroimage 114, 71–87. doi:10.1016/j.neuroimage.2015.04.023. [PubMed: 25896931]

Does MD, 2018. Inferring brain tissue composition and microstructure via MR relaxometry. Neuroimage 182, 136–148. doi:10.1016/j.neuroimage.2017.12.087. [PubMed: 29305163]

Fischl B, 2012. FreeSurfer. Neuroimage 62 (2), 774–781. doi:10.1016/j.neuroimage.2012.01.021. [PubMed: 22248573]

Fukunaga M, Li TQ, van Gelderen P, de Zwart JA, Shmueli K, Yao B, … Duyn JH, 2010. Layer-specific variation of iron content in cerebral cortex as a source of MRI contrast. Proc. Natl. Acad. Sci. USA 107 (8), 3834–3839. doi:10.1073/pnas.0911177107. [PubMed: 20133720]

Ganzetti M, Wenderoth N, Mantini D, 2014. Whole brain myelin mapping using T1- and T2-weighted MR imaging data. Front. Hum. Neurosci. 8, 671. doi:10.3389/fnhum.2014.00671. [PubMed: 25228871]

Glasser MF, Coalson TS, Harms MP, Xu J, Baum GL, Autio JA, … Hayashi T, 2022. Empirical transmit field bias correction of T1w/T2w myelin maps. Neuroimage 258, 119360. doi:10.1016/j.neuroimage.2022.119360. [PubMed: 35697132]

Glasser MF, Coalson TS, Robinson EC, Hacker CD, Harwell J, Yacoub E, … Van Essen DC, 2016. A multi-modal parcellation of human cerebral cortex. Nature 536 (7615), 171–178. doi:10.1038/nature18933. [PubMed: 27437579]

Glasser MF, Goyal MS, Preuss TM, Raichle ME, … Van Essen DC, 2014. Trends and properties of human cerebral cortex: correlations with cortical myelin content. Neuroimage 93, 165–175. doi:10.1016/j.neuroimage.2013.03.060, Pt 2. [PubMed: 23567887]

Glasser MF, Sotiropoulos SN, Wilson JA, Coalson TS, Fischl B, Andersson JL, … Consortium WU-MH., 2013. The minimal preprocessing pipelines for the human connectome project. Neuroimage 80, 105–124. doi:10.1016/j.neuroimage.2013.04.127. [PubMed: 23668970]

Glasser MF, Van Essen DC, 2011. Mapping human cortical areas *in vivo* based on myelin content as revealed by T1- and T2-weighted MRI. J. Neurosci 31 (32), 11597–11616. doi:10.1523/JNEUROSCI.2180-11.2011. [PubMed: 21832190]

Grady CL, Furey ML, Pietrini P, Horwitz B, Rapoport SI, 2001. Altered brain functional connectivity and impaired short-term memory in Alzheimer's disease. Brain 124 (4), 739–756. doi:10.1093/brain/124.4.739, Pt. [PubMed: 11287374]

Grydeland H, Vertes PE, Vasa F, Romero-Garcia R, Whitaker K, Alexander-Bloch AF, … Bullmore ET, 2019. Waves of maturation and senescence in microstructural MRI markers of human cortical myelination over the lifespan. Cereb. Cortex 29 (3), 1369–1381. doi:10.1093/cercor/bhy330. [PubMed: 30590439]

Grydeland H, Walhovd KB, Tamnes CK, Westlye LT, Fjell AM, 2013. Intracortical myelin links with performance variability across the human lifespan: results from T1- and T2-weighted MRI myelin mapping and diffusion tensor imaging. J. Neurosci. 33 (47), 18618–18630. doi:10.1523/JNEUROSCI.2811-13.2013. [PubMed: 24259583]

Hagiwara A, Hori M, Kamagata K, Warntjes M, Matsuyoshi D, Nakazawa M, … Aoki S, 2018. Myelin measurement: comparison between simultaneous tissue relaxometry, magnetization transfer saturation index, and T1w/T2w ratio methods. Sci. Rep 8 (1), 10554. doi:10.1038/s41598-018-28852-6. [PubMed: 30002497]

Harkins KD, Xu J, Dula AN, Li K, Valentine WM, Gochberg DF, … Does MD, 2016 The microstructural correlates of T1 in white matter. Magn. Reson. Med 75 (3), 1341–1345. doi:10.1002/mrm.25709. [PubMed: 25920491]

Harms MP, Somerville LH, Ances BM, Andersson J, Barch DM, Bastiani M, … Yacoub E, 2018. Extending the human connectome project across ages: imaging protocols for the lifespan development and aging projects. Neuroimage 183, 972–984. doi:10.1016/j.neuroimage.2018.09.060. [PubMed: 30261308]

Haroutunian V, Katsel P, Roussos P, Davis K, Altshuler L, Bartzokis G, 2014. Myelination, oligodendrocytes, and serious mental illness. Glia 62 (11), 1856–1877. doi:10.1002/glia.22716 . [PubMed: 25056210]

Heath F, Hurley SA, Johansen-Berg H, Sampaio-Baptista C, 2018. Advances in non-invasive myelin imaging. Dev. Neurobiol 78 (2), 136–151. doi:10.1002/dneu.22552. [PubMed: 29082667]

Huntenburg JM, Bazin PL, Goulas A, Tardif CL, Villringer A, Margulies DS, 2017 A systematic relationship between functional connectivity and intracortical myelin in the human cerebral cortex. Cereb. Cortex 27 (2), 981–997. doi:10.1093/cer-cor/bhx030. [PubMed: 28184415]

Jenkinson M, Beckmann CF, Behrens TE, Woolrich MW, Smith SM, 2012. FSL. Neuroimage 62 (2), 782–790. doi:10.1016/j.neuroimage.2011.09.015. [PubMed: 21979382]

Kemper TL (1994). Neuroanatomical and neuropathological changes during aging and dementia.

Kiernan J, Rajakumar R, 2013. Barr's the Human Nervous System: An Anatomical Viewpoint. Lippincott Williams & Wilkins .

Lintl P, Braak H, 1983. Loss of intracortical myelinated fibers: a distinctive age-related alteration in the human striate area. Acta Neuropathol. 61 (3), 178–182. doi:10.1007/BF00691983, -4. [PubMed: 6650131]

Mezer A, Yeatman JD, Stikov N, Kay KN, Cho NJ, Dougherty RF, … Wandell BA, 2013. Quantifying the local tissue volume and composition in individual brains with magnetic resonance imaging. Nat. Med 19 (12), 1667–1672. doi:10.1038/nm.3390. [PubMed: 24185694]

Michailov GV, Sereda MW, Brinkmann BG, Fischer TM, Haug B, Birchmeier C, … Nave KA, 2004. Axonal neuregulin-1 regulates myelin sheath thickness. Science 304 (5671), 700–703. doi:10.1126/science.1095862. [PubMed: 15044753]

Micheva KD, Wolman D, Mensh BD, Pax E, Buchanan J, Smith SJ, Bock DD, 2016. A large fraction of neocortical myelin ensheathes axons of local inhibitory neurons. eLife 5. doi:10.7554/eLife.15784.

Miller DJ, Duka T, Stimpson CD, Schapiro SJ, Baze WB, McArthur MJ, … Wildman DE, 2012. Prolonged myelination in human neocortical evolution. Proc. Natl. Acad. Sci 109 (41), 16480–16485. Retrieved from https://www.ncbi.nlm.nih.gov/pmc/articles/PMC3478650/pdf/pnas.201117943.pdf [PubMed: 23012402]

Misaki M, Savitz J, Zotev V, Phillips R, Yuan H, Young KD, … Bodurka J, 2015. Contrast enhancement by combining T1- and T2-weighted structural brain MR Images. Magn. Reson. Med 74 (6), 1609–1620. doi:10.1002/mrm.25560. [PubMed: 25533337]

Nakamura K, Chen JT, Ontaneda D, Fox RJ, Trapp BD, 2017. T1-/T2-weighted ratio differs in demyelinated cortex in multiple sclerosis. Ann. Neurol 82 (4), 635–639. [PubMed: 28833377]

Natu VS, Gomez J, Barnett M, Jeska B, Kirilina E, Jaeger C, … Grill-Spector K, 2019. Apparent thinning of human visual cortex during childhood is associated with myelination. Proc. Natl. Acad. Sci. USA 116 (41), 20750–20759. doi:10.1073/pnas.1904931116. [PubMed: 31548375]

Nieuwenhuys R, 2013. The myeloarchitectonic studies on the human cerebral cortex of the Vogt-Vogt school, and their significance for the interpretation of functional neuroimaging data. Brain Struct. Funct. 218 (2), 303–352. doi:10.1007/s00429-012-0460-z.

O'Brien JS, Sampson EL, 1965. Lipid composition of the normal human brain: gray matter, white matter, and myelin. J. Lipid Res 6 (4), 537–544. Retrieved from https://www.ncbi.nlm.nih.gov/pubmed/5865382 . [PubMed: 5865382]

Ogg RJ, Steen RG, 1998. Age-related changes in brain T1 are correlated with iron concentration. Magn. Reson. Med 40 (5), 749–753. doi:10.1002/mrm.1910400516. [PubMed: 9797159]

Papuc E, Rejdak K, 2020. The role of myelin damage in Alzheimer's disease pathology. Arch. Med. Sci 16 (2), 345–351. doi:10.5114/aoms.2018.76863. [PubMed: 32190145]

Paquola C, Bethlehem RA, Seidlitz J, Wagstyl K, Romero-Garcia R, Whitaker KJ, … Bullmore ET, 2019. Shifts in myeloarchitecture characterise adolescent development of cortical gradients. eLife 8. doi:10.7554/eLife.50482 .

Paquola C, Vos De Wael R, Wagstyl K, Bethlehem RAI, Hong SJ, Seidlitz J, … Bernhardt BC, 2019. Microstructural and functional gradients are increasingly dissociated in transmodal cortices. PLoS Biol. 17 (5), e3000284. doi:10.1371/jour-nal.pbio.3000284. [PubMed: 31107870]

Pelkmans W, Dicks E, Barkhof F, Vrenken H, Scheltens P, van der Flier WM, Tijms BM, 2019. Gray matter T1-w/T2-w ratios are higher in Alzheimer's disease. Hum. Brain Mapp 40 (13), 3900–3909. doi:10.1002/hbm.24638. [PubMed: 31157938]

Peters A, 2002. The effects of normal aging on myelin and nerve fibers: a review. J. Neurocytol 31 (8-9), 581–593. doi:10.1023/a:1025731309829 . [PubMed: 14501200]

Peters A, 2009. The effects of normal aging on myelinated nerve fibers in monkey central nervous system. Front. Neuroanat 3, 11. doi:10.3389/neuro.05.011.2009. [PubMed: 19636385]

Petracca M, El Mendili MM, Moro M, Cocozza S, Podranski K, Fleysher L, Inglese M, 2020. Laminar analysis of the cortical T1/T2-weighted ratio at 7T. Neurol. Neuroimmunol. Neuroinflamm 7 (6). doi:10.1212/NXI.0000000000000900.

Righart R, Biberacher V, Jonkman LE, Klaver R, Schmidt P, Buck D, … Muhlau M, 2017. Cortical pathology in multiple sclerosis detected by the T1/T2-weighted ratio from routine magnetic resonance imaging. Ann. Neurol 82 (4), 519–529. doi:10.1002/ana.25020. [PubMed: 28833433]

Rowley CD, Bazin PL, Tardif CL, Sehmbi M, Hashim E, Zaharieva N, …Bock NA, 2015. Assessing intracortical myelin in the living human brain using myelinated cortical thickness. Front. Neurosci 9, 396. doi:10.3389/fnins.2015.00396. [PubMed: 26557052]

Schaefer A, Kong R, Gordon EM, Laumann TO, Zuo XN, Holmes AJ, … Yeo BTT, 2018. Local-global parcellation of the human cerebral cortex from intrinsic functional connectivity MRI. Cereb. Cortex 28 (9), 3095–3114. doi:10.1093/cer-cor/bhx179. [PubMed: 28981612]

Seifert AC, Umphlett M, Hefti M, Fowkes M, Xu J, 2019. Formalin tissue fixation biases myelin-sensitive MRI. Magn. Reson. Med 82 (4), 1504–1517. doi:10.1002/mrm.27821. [PubMed: 31125149]

Shafto MA, Tyler LK, Dixon M, Taylor JR, Rowe JB, Cusack R, … Cam CAN, 2014. The Cambridge Centre for Ageing and Neuroscience (Cam-CAN) study protocol: a cross-sectional, lifespan, multidisciplinary examination of healthy cognitive ageing. BMC Neurol 14, 204. doi:10.1186/s12883-014-0204-1. [PubMed: 25412575]

Shams Z, Norris DG, Marques JP, 2019. A comparison of *in vivo* MRI based cortical myelin mapping using T1w/T2w and R1 mapping at 3T. PLoS One 14 (7), e0218089. doi:10.1371/journal.pone.0218089. [PubMed: 31269041]

Shatil AS, Uddin MN, Matsuda KM, Figley CR, 2018. Quantitative *ex vivo* MRI changes due to progressive formalin fixation in whole human brain specimens: longitudinal characterization of diffusion, relaxometry, and myelin water fraction measurements at 3T. Front. Med. (Lausanne) 5, 31. doi:10.3389/fmed.2018.00031. [PubMed: 29515998]

Shaw ME, Sachdev PS, Anstey KJ, Cherbuin N, 2016. Age-related cortical thinning in cognitively healthy individuals in their 60s: the PATH through life study. Neurobiol. Aging 39, 202–209. doi:10.1016/j.neurobiolaging.2015.12.009. [PubMed: 26923417]

Sprooten E, O'Halloran R, Dinse J, Lee WH, Moser DA, Doucet GE, … Frangou S, 2019. Depth-dependent intracortical myelin organization in the living human brain determined by

in vivo ultra-high field magnetic resonance imaging. Neuroimage 185, 27–34. doi:10.1016/ j.neuroimage.2018.10.023. [PubMed: 30312809]

Streckenbach F, Stachs O, Langner S, Guthoff RF, Meinel FG, Weber MA, … Beller E, 2020. Age-related changes of the human crystalline lens on high-spatial resolution three-dimensional T1-weighted brain magnetic resonance images *in vivo.* Investig. Ophthalmol. Vis. Sci 61 (14), 7. doi:10.1167/iovs.61.14.7 .

Stuber C, Morawski M, Schafer A, Labadie C, Wahnert M, Leuze C, … Turner R, 2014. Myelin and iron concentration in the human brain: a quantitative study of MRI contrast. Neuroimage 93, 95–106. doi:10.1016/j.neuroimage.2014.02.026, Pt 1. [PubMed: 24607447]

Sui YV, Bertisch H, Lee HH, Storey P, Babb JS, Goff DC, … Lazar M, 2021. Quantitative macromolecular proton fraction Mapping reveals altered cortical myelin profile in schizophrenia spectrum disorders. Cereb Cortex Commun. 2 (2). doi:10.1093/texcom/tgab015, tgab015.

Taylor JR, Williams N, Cusack R, Auer T, Shafto MA, Dixon M, … Henson RN, 2017. The Cambridge Centre for Ageing and Neuroscience (Cam-CAN) data repository: structural and functional MRI, MEG, and cognitive data from a cross-sectional adult lifespan sample. Neuroimage 144, 262–269. doi:10.1016/j.neuroimage.2015.09.018, Pt B. [PubMed: 26375206]

Uddin MN, Figley TD, Solar KG, Shatil AS, Figley CR, 2019. Comparisons between multi-component myelin water fraction, T1w/T2w ratio, and diffusion tensor imaging measures in healthy human brain structures. Sci. Rep 9 (1), 2500. doi:10.1038/s41598-019-39199-x, -2500. [PubMed: 30792440]

Vidal-Pineiro D, Walhovd KB, Storsve AB, Grydeland H, Rohani DA, Fjell AM, 2016 Accelerated longitudinal gray/white matter contrast decline in aging in lightly myelinated cortical regions. Hum. Brain Mapp 37 (10), 3669–3684. doi:10.1002/hbm.23267. [PubMed: 27228371]

Wei Y, Collin G, Mandl RCW, Cahn W, Keunen K, Schmidt R, … van den Heuvel MP, 2018. Cortical magnetization transfer abnormalities and connectome dysconnectivity in schizophrenia. Schizophr. Res 192, 172–178. doi:10.1016/j.schres.2017.05.029. [PubMed: 28601503]

Westlye LT, Walhovd KB, Dale AM, Espeseth T, Reinvang I, Raz N, … Fjell AM, 2009. Increased sensitivity to effects of normal aging and Alzheimer's disease on cortical thickness by adjustment for local variability in gray/white contrast: a multi-sample MRI study. Neuroimage 47 (4), 1545– 1557. doi:10.1016/j.neuroimage.2009.05.084. [PubMed: 19501655]

Yarnykh VL, 2012. Fast macromolecular proton fraction mapping from a single off-resonance magnetization transfer measurement. Magn. Reson. Med 68 (1), 166–178. doi:10.1002/ mrm.23224. [PubMed: 22190042]

Yasuno F, Kazui H, Morita N, Kajimoto K, Ihara M, Taguchi A, … Nagatsuka K, 2017 Use of T1-weighted/T2-weighted magnetic resonance ratio to elucidate changes due to amyloid beta accumulation in cognitively normal subjects. Neuroimage Clin. 13, 209–214. doi:10.1016/ j.nicl.2016.11.029. [PubMed: 28003959]

Yeatman JD, Wandell BA, Mezer AA, 2014. Lifespan maturation and degeneration of human brain white matter. Nat. Commun 5, 4932. doi:10.1038/ncomms5932. [PubMed: 25230200]

Yeo BT, Krienen FM, Sepulcre J, Sabuncu MR, Lashkari D, Hollinshead M, … Buckner RL, 2011. The organization of the human cerebral cortex estimated by intrinsic functional connectivity. J. Neurophysiol 106 (3), 1125–1165. doi:10.1152/jn.00338.2011. [PubMed: 21653723]

Yoshiura T, Higano S, Rubio A, Shrier DA, Kwok WE, Iwanaga S, Nu-maguchi Y, 2000. Heschl and superior temporal gyri: low signal intensity of the cortex on T2-weighted MR images of the normal brain. Radiology 214 (1), 217–221. doi:10.1148/radiology.214.1.r00ja17217. [PubMed: 10644127]

Zatorre RJ, Fields RD, Johansen-Berg H, 2012. Plasticity in gray and white: neuroimaging changes in brain structure during learning. Nat. Neurosci 15 (4), 528–536. doi:10.1038/nn.3045. [PubMed: 22426254]
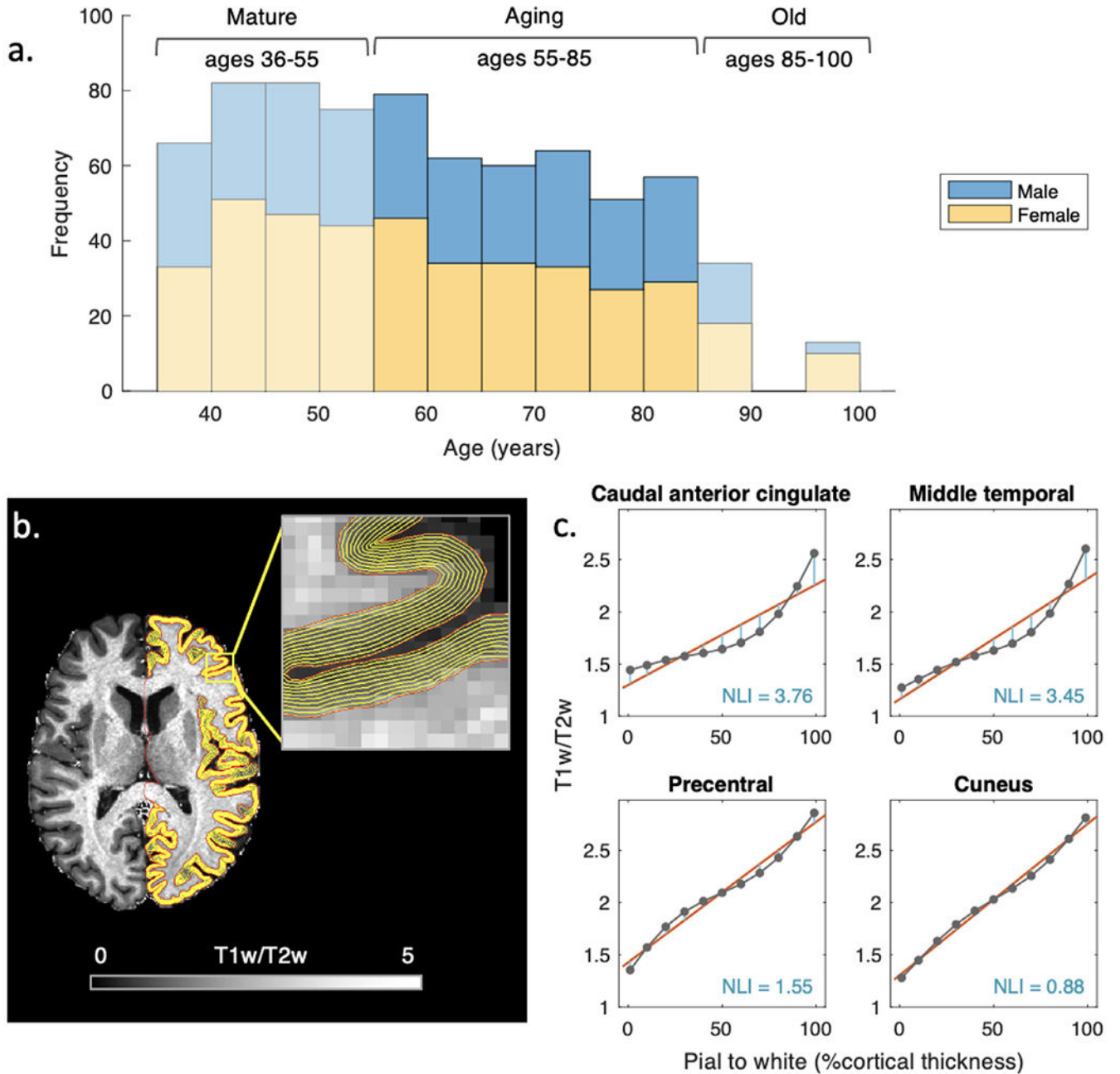
Fig. 1.

(a) Human Connectome Project in Aging (HCP-A) dataset age distribution separated by sex. The ages 55 to 85, which were used for examining typical aging in the current study, are highlighted; (b) Example T1w/T2w ratio image of one participant in axial view. The pial and white surface of the left hemisphere are marked red. The expanded 11 surfaces are drawn in yellow; (c) Cortical T1w/T2w profiles of selected regions of interest (ROIs) in the left hemisphere of one example participant. Regions are selected to show cortical profiles of varying nonlinearity index (NLI) levels. Mean T1w/T2w values at different cortical depth of each ROI are plotted as gray dots with the linear fitting line drawn in orange.
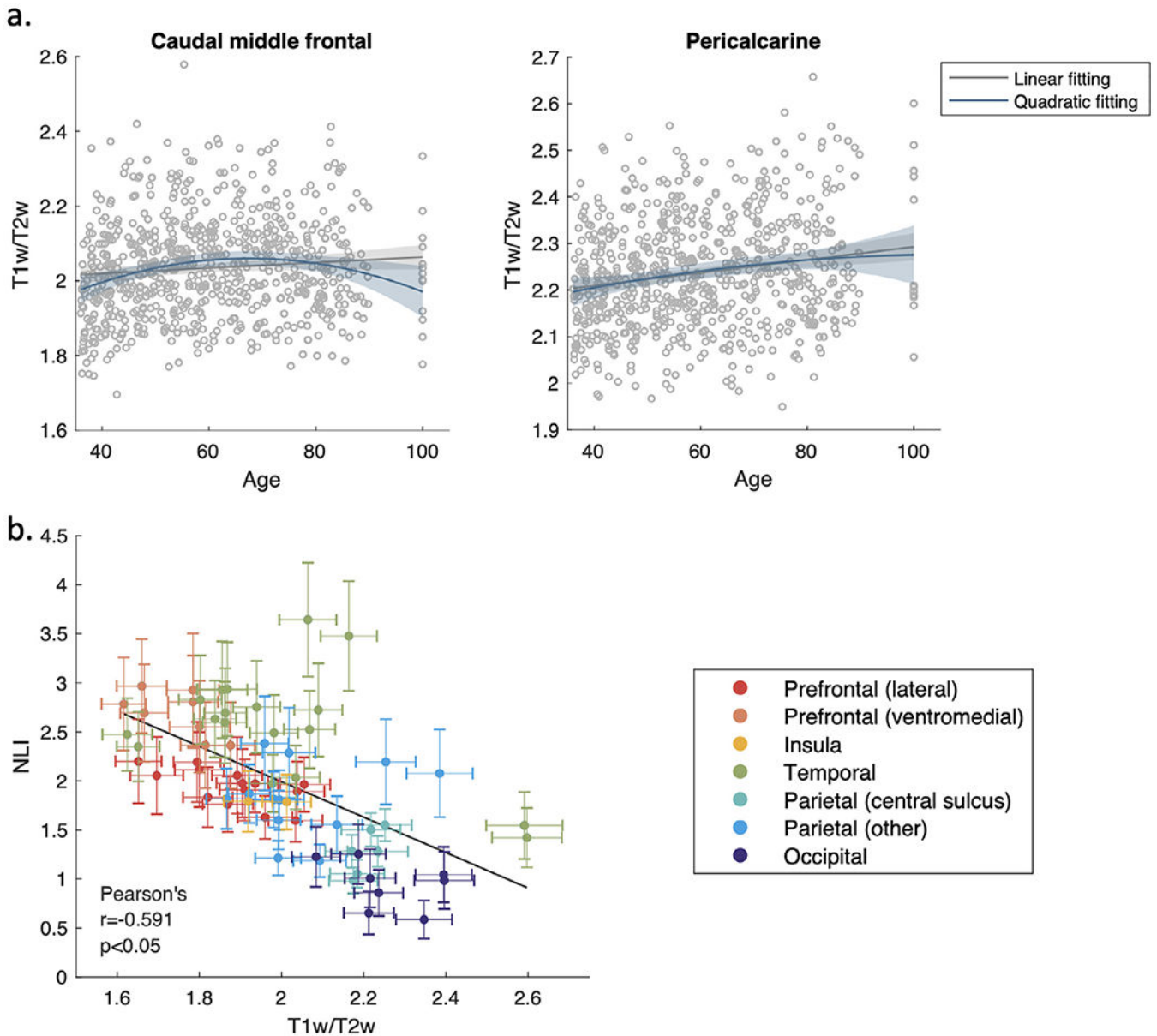
Fig. 2.
(a) T1w/T2w trajectories in example regions (significant quadratic age effect in left caudal middle frontal and significant linear age effect only in left precentral region) across age groups (for full results see Supplementary Table S2, Fig. S4). T1w/T2w ratio values are extracted from 70% cortical thickness depth from the pial surface for comparison with previous results (Grydeland et al., 2013). Linear and quadratic fitting lines and corresponding 95% confidence intervals are shown; (b) Scatter plot of regional nonlinearity index (NLI) values against the 70% depth T1w/T2w ratio across age groups, color coded by cortical area. Error bars show $\frac{1}{2}$ of each metrics' standard deviation (SD) across the whole sample. The entire length of the error bar represents one SD range.
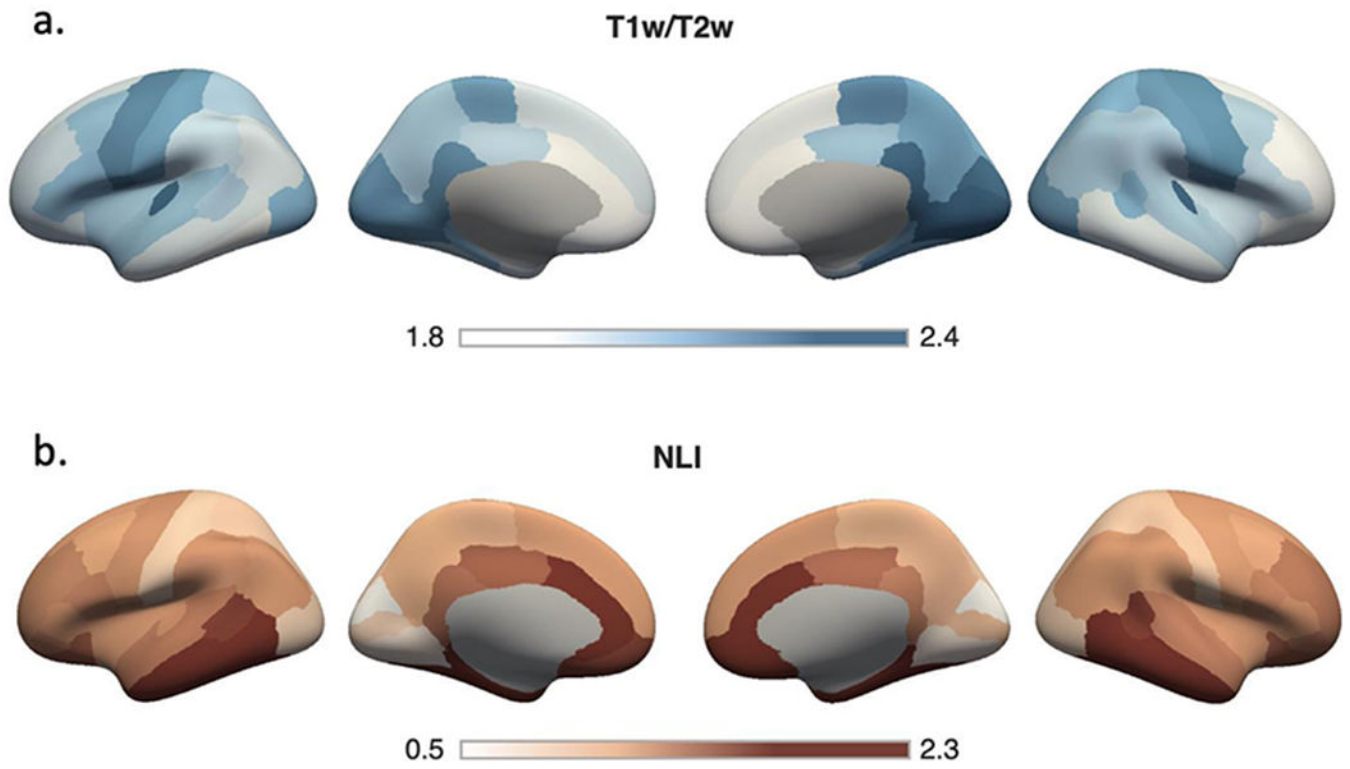
Fig. 3.

Average regional T1w/T2w ratio at 70% cortical depth (a) and nonlinearity index (NLI; b) across cortical regions of interest in the aging (ages 55-85) group.
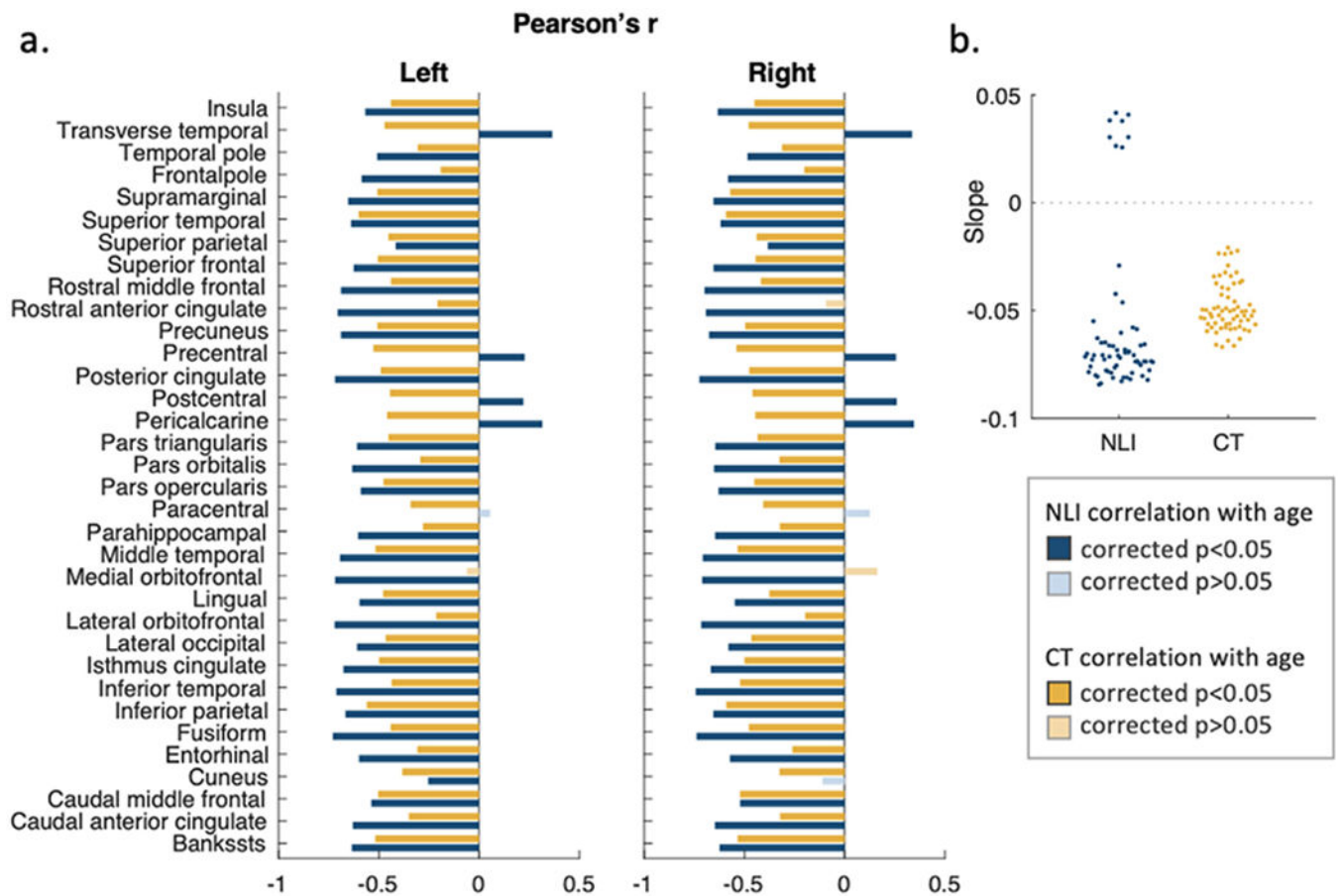
Fig. 4.
Nonlinearity index (NLI; blue color scheme) and cortical thickness (CT; yellow color scheme) associations with age in the aging group, controlling for participants' sex and body mass index. (a) Bar plots show the Pearson's correlation coefficient r for the relationship with age in regional NLI and CT. The shade of the bar color reflects statistical significance after multiple comparison correction; (b) the slopes of linear fitting lines of standardized NLI and CT changes with age across cortical regions. Only those with significant relationships are shown.
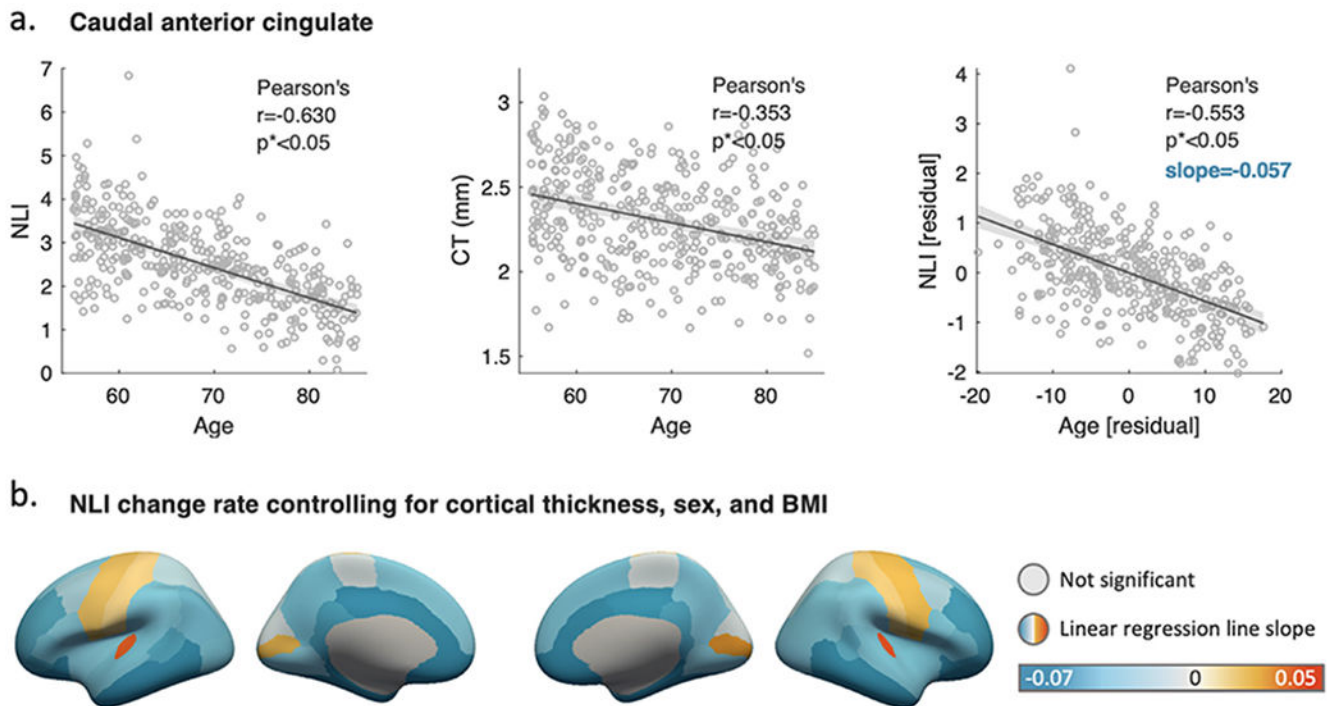
Fig. 5.

(a) Scatter plots describing the relationship between the nonlinearity index (NLI), cortical thickness (CT) and age in an example region (left caudal anterior cingulate). Far right shows the partial plot of NLI against age controlling for participants' sex, body mass index (BMI), and regional CT. Pearson's correlation coefficient r and corrected p-values (p^*) are shown. Shaded areas indicate 95% confidence intervals; (b) The slopes of linear fitting lines of the NLI as a function of age, controlling for participants' sex, body mass index (BMI), and regional CT. Color reflects slope values for significant partial correlations (e.g., darker blue indicates faster NLI decline with age controlling for covariates).
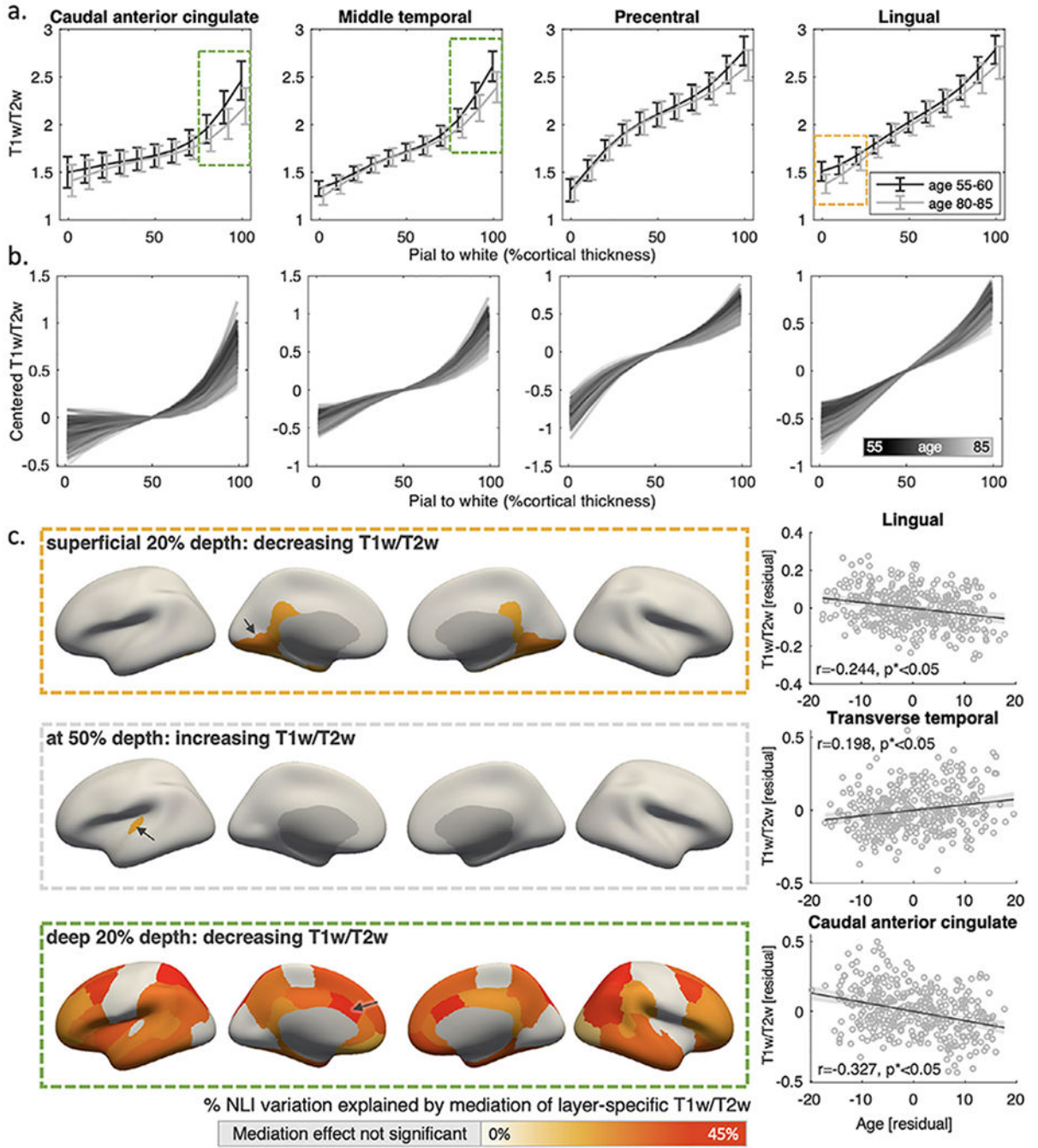
Fig. 6.

Differences in T1w/T2w ratio at specific depth behind profile nonlinearity index (NLI) variations. (a) Average T1w/T2w profiles of those aged 55-60 (black) and 80-85 (grey) shown for representative regions of interest (Fig. 1c) to highlight differences in profiles. Error bars indicate one standard deviation range; (b) Individual T1w/T2w profiles colored by participants' age. To better visualize T1w/T2w profile variations with age, individual profiles are superimposed (with 30% transparency) and centered to mean T1w/T2w values at 50% cortical depth; (c) Percentage of age-related NLI variation that is explained by the

mediation effect of average T1w/T2w values from specific surfaces (superficial/deep 20% depths, and at 50% depth). Variations due to participants' sex, body mass index (BMI), and regional cortical thickness (CT) are controlled. Partial plots of depth-specific T1w/T2w values against age in example regions, indicated by black arrows in the brain surface graphs, are shown on the right. Pearson's correlation coefficient r and corrected p-values (p*) are included. Shaded areas in scatter plots indicate 95% confidence intervals.

Table 1

Demographics by age groups.

	Mature (Younger than 55)	Aging (Between 55 and 85)	Old (85 and above)
N	305	375	45
Sex (M/F)	130/175	171/204	18/27
Age			
mean (SD)	45.3 (5.7)	68.8 (8.8)	90.9 (6.0)
[range]	[36.0-54.9]	[55.2-84.9]	[85.1-100.0]
BMI			
mean (SD)	27.5 (5.1)	26.6 (4.5)	25.5 (3.5)
[range]	[18.3-41.8]	[15.7-43.7]	[19.3-34.3]